ACADEMIA ROMÂNĂ
Revue Roumaine de Chimie
http://web.icf.ro/rrch/

Rev. Roum. Chim.,
2021, *66*(3), 219–229
DOI: 10.33224/rrch.2021.66.3.01

Papers

Dedicated to the memory of
Professor Dumitru OANCEA (1941–2020)

THERMAL BEHAVIOR OF Cu-DOPED TiO_2 GELS SYNTHESIZED BY THE SOL-GEL METHOD

Jeanina PANDELE-CUSU,[a] Irina ATKINSON,[a] Adriana RUSU,[a] Nicoleta APOSTOL,[b] Valentin TEODORESCU,[b] Luminita PREDOANA,[a] Imre M. SZILÁGYI,[c] György POKOL[c,d] and Maria ZAHARESCU[*]

[a]"Ilie Murgulescu" Institute of Physical Chemistry of the Roumanian Academy, 202 Spl. Independentei, 060021 Bucharest, Roumania
[b]National Institute of Materials Physics, 405 bis Atomistilor Street, 077125 Magurele-Ilfov, Roumania
[c]Department of Inorganic and Analytical Chemistry Budapest University of Technology and Economics, H-1111 Budapest, Műegyetem rakpart 3, Hungary
[d]Research Center for Natural Sciences, Hungarian Academy of Science 1117 Budapest, Magyar tudósokkörútja 2, Hungary

Received October 21, 2020

The thermal behavior of Cu-doped TiO_2 gels obtained by the sol-gel method was investigated by thermogravimetric and differential thermal analysis (TG/DTG/DTA) and differential scanning calorimetry (DSC) measurements. The comparative investigation of the structure and morphology of the as-prepared gels and of the nanopowders obtained by annealing them was realized by transmission electron microscopy (TEM), Fourier transmission infrared spectroscopy (FTIR), X-ray diffraction (XRD) and X-ray photoelectron spectroscopy (XPS). Significant differences were noticed depending on the amount of dopant (0.5 or 2.0 mol % CuO). A higher dopant concentration resulted in a more complex decomposition of the sample. This behavior was associated with the formation of various molecular species in the sol-gel solutions before gelation, determined by the different amount of the dopant used.

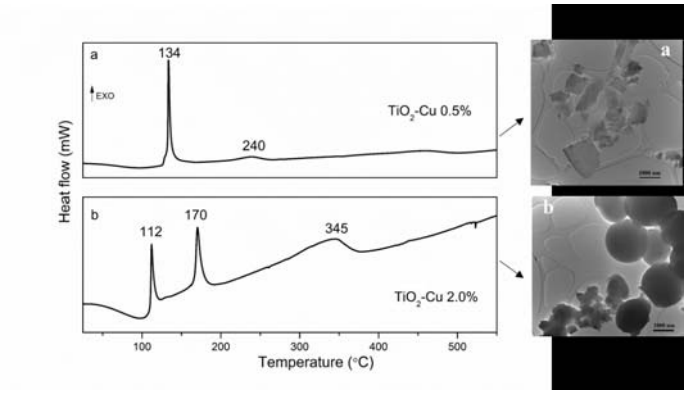

INTRODUCTION

Since the "nano era" started,[1] the most studied oxide in nanometric size has been TiO_2. TiO_2 is an ***n***-type semiconductor with a large band gap (3.2 eV for anatase and 3.0 eV for rutile phase) and a long lifetime of photo-excited electrons.[2,3] It has several remarkable properties, such as non-toxicity, exceptional resistance to corrosion, physical and chemical stability, good optical properties, high photocatalytic activity, and low cost. Up to date, the nanostructured TiO_2 was successfully applied in fields such as photocatalysis,[4] gas sensors,[5] dye sensitized solar

[*] Corresponding author: mzaharescu2004@yahoo.com

cells,[6] optical coatings, antimicrobial materials,[7] pigments, etc.

To improve the properties of TiO_2, respectively to increase its functionality within the frame of the desired application, various dopants have been proposed. Among them, an increased interest is given to doping with the Al^{3+} and transition metal ions (for example: Fe^{3+}, Co^{3+}, $V^{4+/5+}$, Nb^{5+}, $Mo^{5+/6+}$, Ag^{+}, Pt^{4+}, Cu^{+}), as well as to certain lanthanides and actinides: (La^{3+}, Ce^{3+}, Er^{3+}, Ru^{3+}, Pr^{3+}, Gd^{3+}, Nd^{3+}, Sm^{3}).[8-16] Transition metal ions are the most popular dopants because they have partially filled **d** orbitals. Doping with various metals or non-metals has been extensively explored as a way to narrow TiO_2 bandgap and to enhance its photocatalytic activity under visible light. Using Cu as a dopant is a cheap and affordable alternative, and it can form an additional band.[17-21]

For the preparation of TiO_2 or doped TiO_2 materials different methods are available. Among them, the sol-gel method is often used to synthesize doped TiO_2 because it has advantages such as high purity, relatively low processing temperature and offers the possibility of controlling stoichiometry.[9, 21-27]

In the case of Cu doped TiO_2 system previous papers were published. In these papers low amount of Cu and mainly inorganic Cu reagents were used, as the following: copper (II) trioxonitrate (V) (0.033 g),[19] copper sulphate pentahydrate (0.5 mol %),[20] copper (II) chloride anhydrous (1 mol.%)[22] or copper chloride dihydrate (0 to 6 at. %)[23] and cooper (II) nitrate/$Me(NO_3)x$/TIP = 0.015 molar ratio.[24]

In the present paper, the sol-gel preparation of Cu doped TiO_2 nanometric powders is discussed, as well as the influence of the amount of dopant on the thermal behavior of the synthesized samples and on the structure and properties of the resulted nanopowders. As compared to the literature data, the Cu amount in our investigation was in the range mentioned in literature, but the reagent used was an organic one (Cu acetylacetonate).

EXPERIMENTAL

Gels and powders preparation

The Cu-doped TiO_2 powders were prepared by the sol-gel method. The initial calculated compositions correspond to a TiO_2:CuO molar percentage of 98:2.0 and 99.5:0.5, respectively. The titanium tetraisopropoxide (Du Pont) [TTIP = $Ti(O\text{-}i\text{-}C_3H_7)_4$] and Cu acetylacetonate $Cu(Acac)_2$ (Sigma-Aldrich) – [$C_{10}H_{14}CuO_4$] were used as starting precursors in isopropanol medium. Acetylacetone (AcAc) (Sigma-Aldrich) [$C_5H_8O_2$] was used as chelating agent. Nitric acid (Merck) [HNO_3] was used as catalyst. The obtained reaction mixtures were homogenized at room temperature for 2 hours, then dried at 100°C for 12 h to prepare the gel samples, followed by a thermal treatment for 1 h at 400°C with a heating rate of 1°C/min, in order to eliminate the water and organic residues and to obtain crystallized nanometric powders. The thermal treatment was established based on the TG/DTG/DTA results.

The synthesized powders were labeled (TiO_2–Cu 0.5%) and (TiO_2–Cu 2.0%), respectively.

The composition of the initial solutions and the experimental conditions used are presented in Table 1.

Methods of gels and powders characterization

The **thermal behavior** of the as-prepared samples was determined by **thermogravimetric and differential thermal analysis (TG/DTG/DTA)** using Mettler Toledo TGA/SDTA 851^e equipment in open Al_2O_3 crucibles and in flowing air atmosphere. The maximum temperature was set at 1000°C and the heating rate was of 10°C/min.

Differential scanning calorimetry (DSC) measurements were carried out in a DSC 3 Mettler Toledo differential calorimeter, in closed aluminium crucibles with a pinhole in the lead to prevent pressure and build up due do gaseous products. The maximum temperature was set at 600°C with the heating rate of 10°C/min and the purge gas was nitrogen.

The **transmission electron microscopy (TEM)** observations were done using the JEOL ARM200F analytical electron microscope, working at 200 kV.

Table 1

Composition of the initial solution and the experimental conditions of sol preparation

Sample	Reagents	Molar ratio				pH sol	Experimental conditions	
		TiO_2/CuO	$\frac{ROH}{\sum precursor}$	$\frac{H_2O}{\sum precursor}$	$\frac{catalyst}{\sum precursor}$		T (°C)	t (h)
TiO_2-Cu 0.5%	$Ti(OC_3H_7)_4$ + $Cu(Acac)_2$	99.5/0.5	36.5	1.35	0.35	3.5	25	2
TiO_2-Cu 2.0%	$Ti(OC_3H_7)_4$ + $Cu(Acac)_2$	98/2.0	36.5	1.35	0.35	3.5	25	2

ROH = C_3H_7-OH

The **Fourier-transform infrared** (FT-IR) spectra of the as-prepared samples and powders resulted after thermal treatment were obtained using a Nicolet Spectrometer 6700 FT-IR between 400 and 4000 cm^{-1}. The spectra were collected using the KBr pellet technique. For each sample the spectra were recorded at a resolution of 4 cm^{-1} and processed using the OMNIC 7.3 software.

The **X-ray measurements (XRD)** were performed with an Ultima IV X-Ray Diffractometer (Rigaku, Japan) using the Cu Kα radiation (Kα = 1.54056 Å) with a scan rate of 2^o/min and 0.02^o step size, at 40 kV and 30 mA. The diffraction pattern ranging between 10^o and 80^o was recorded.

The samples' surface was investigated by **X-Ray Photoelectron Spectroscopy (XPS)** performed with an AXIS Ultra DLD (Kratos Surface Analysis) setup, using Mg Kα (1253,4 eV) radiation produced by a non-monochromatized X-Ray source at operating power of 120 W (12 kV×10 mA). Partial charge compensation was reached by using a flood gun operating at 1.5 A filament current, 2.7 V charge balance, 1.0 V filament bias. High resolution core level spectra have been recorded using hybrid lens mode, 40 eV pass energy slot aperture.

RESULTS AND DISCUSSION

The samples obtained in the conditions presented above were investigated for their structure, morphology and thermal behavior. In the case of the sample doped with 0.5% mol CuO a brown gel is formed, while the sample containing 2.0% mol CuO transforms into an amorphous yellow powder.

As-prepared gels

The FT-IR spectra of Cu doped TiO_2 as-prepared samples are shown in Fig. 1 and the corresponding vibration bands are presented comparatively in the Table 2.

In both studied samples the same vibration bands are identified, but with different intensity.

The broad absorption bands between 3420 cm^{-1} and 3200 cm^{-1} indicate the presence of the hydroxyl groups, while the vibration band at 2962 cm^{-1} is assigned to the presence of C-H, $\nu_{as}(CH)_3$. The vibration band around 2428 cm^{-1} is attributed to physical CO_2 gas absorbed at the surface of material.[28,29] The sample with 0.5% Cu shows the presence of a high amount of hydroxyl groups in its composition, while the sample with 2.0 % Cu contains a higher amount of organic components confirmed by the presence of the vibration band at 2962 cm^{-1} and much lower intensity of the hydroxyl vibration bands.

The band at about 1386 cm^{-1} is the typical vibration band of the NO_3^- , while the band at 1638 cm^{-1} is related to the bending vibration of the molecular water. The vibration bands corresponding to organic part of the reagents are observed between 1250 and 1000 cm^{-1}.

The vibration band attributed to O-Metal (M)-O is observed at 790 cm^{-1}. The vibration bands related to M-O framework (Ti-O and Cu-O) are noticed at 559 and 479 cm^{-1}.

The surface of the samples and the oxidation states of the components were investigated by **X-Ray Photoelectron Spectroscopy (XPS).** All the core level spectra of interest (Ti 2p, O 1s and Cu 2p) have been deconvoluted using Voigt profiles, based on the methods described in reference.[30] The atomic composition has been determined by using the integral areas provided by the deconvolution procedure normed to the atomic sensitivity factors provided by reference.[31] The XPS spectra deconvoluted with Voigt profiles are illustrated in Fig. 2. For better visualization the baseline for the core level Cu $2p_{3/2}$ was extracted and the main parameters are presented in Table 3.

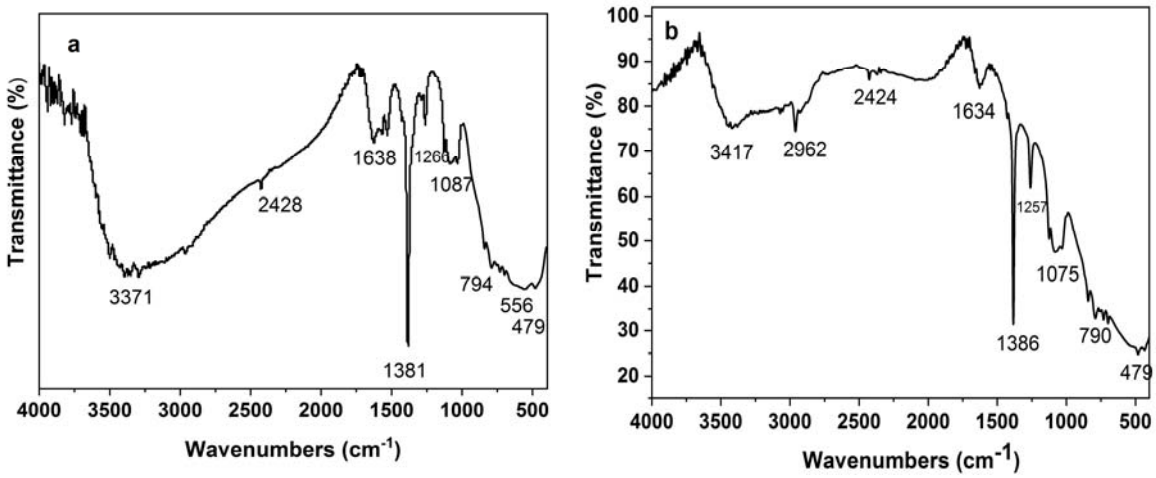

Fig. 1 – IR spectra of the synthesized Cu-doped TiO_2 gels, a) TiO_2-Cu 0.5%, b) TiO_2-Cu 2.0%.

Table 2

The assignment of the vibration bands in IR spectra of the samples

Wavenumber/cm^{-1}		Assignments and vibration mode
TiO_2-Cu 0.5% gel	TiO_2-Cu 2.0% gel	
3371	3417	νOH structural OH group
	2962	C-H, $\nu_{as}(CH)_3$
2428	2424	CO_2 absorption
1638	1634	δH_2O adsorbed water
1381	1386	νNO_3^-
1266	1257	δCH_3
1087	1075	C-O
794	790	O-M-O
556	559	Cu-O, νTi-O
479	479	Cu-O, Ti-O-Ti

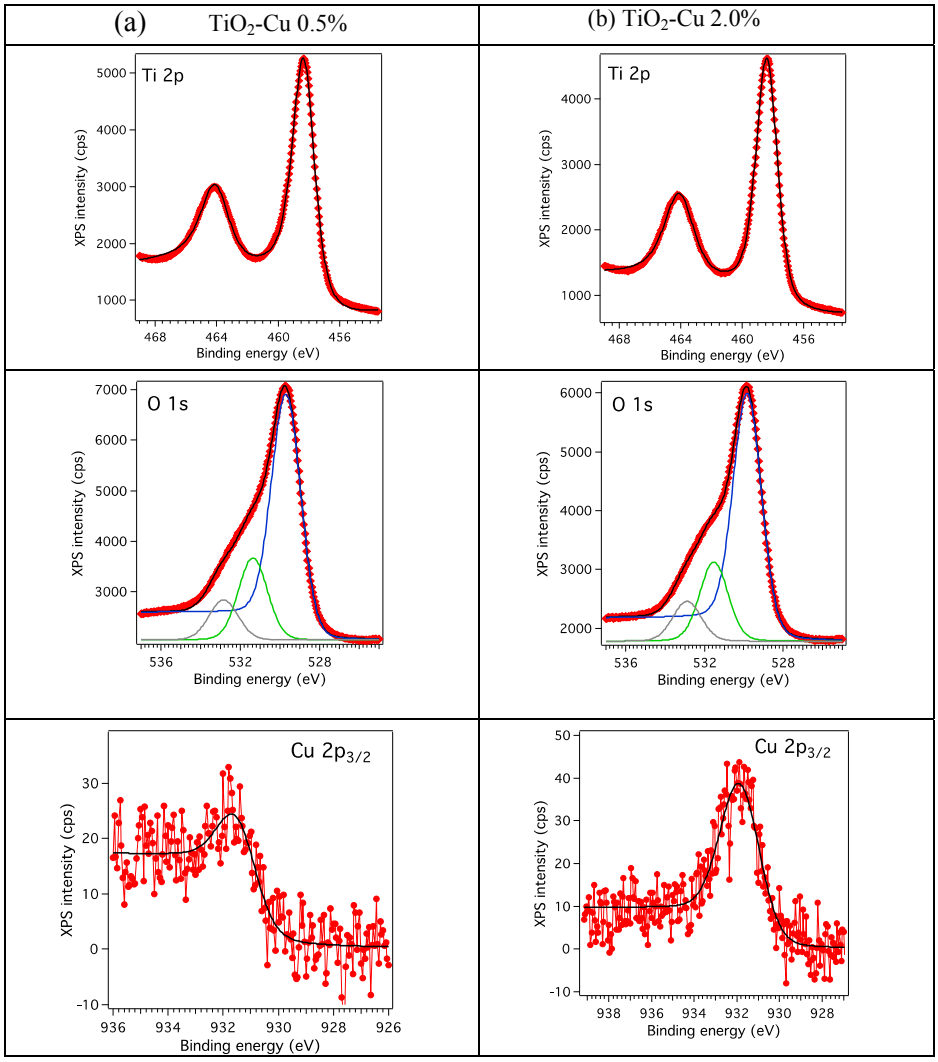

Fig. 2 – XPS spectra of the core level Ti 2p, O 1s and Cu $2p_{3/2}$ for the a) TiO_2-Cu 0.5% and b) TiO_2-Cu 2.0% as-prepared samples.

From the XPS spectra we can see that Ti $2p_{3/2}$ exhibits an intense peak at ~ 458.4 eV and Ti $2p_{1/2}$ at ~ 464.1 which is attributed to TiO_2. The O 1s was deconvoluted with 3 components, the first two, at 529.68 eV and 531.36 eV, constitute the O-Ti, the surface and the "volume" components of TiO_2, and the small component is due to contamination. The Cu $2p_{3/2}$ spectra present a peak at ~ 932 eV, attributed to Cu^+, as it was found in the NIST (National Institute of Standards and Technology) database and in reference. [20]

Table 3

Main parameters obtained from XPS of the samples whose spectra are presented in Fig. 2

Sample	Element		BE (eV)	% at	Interpretation
TiO_2-Cu 0.5%, gel	Ti 2p	C1	458.32	37.66	TiO_2
	O1s	C1	529.68	40.83	TiO_2 vol.
		C2	531.36	14.43	TiO_2 surface
		C3	532.84	7.06	contamination
	Cu $2p_{3/2}$	C1	931.42	0.02	Cu(I)
TiO_2-Cu 2.0%, gel	Ti 2p	C1	458.40	37.62	TiO_2
	O1s	C1	529.81	41.37	TiO_2 vol.
		C2	531.52	13.92	TiO_2surface
		C3	532.89	7.02	contamination
	Cu $2p_{3/2}$	C1	931.82	0.07	Cu(I)

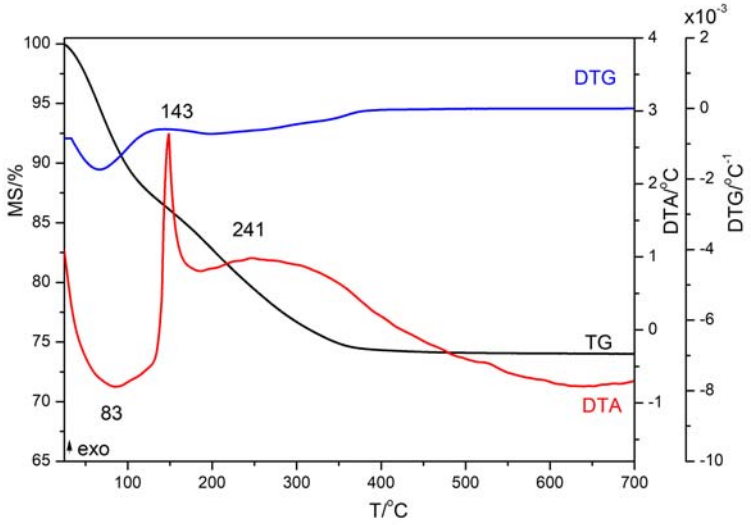

Fig. 3 – TG/DTG/DTA curves of the TiO_2-Cu 0.5% sample.

In order to establish the influence of the samples composition on the thermal behavior, the **thermogravimetric and differential thermal analysis (TG/DTG/DTA)** and as well as **the differential scanning calorimetry (DSC)** were used.

The TG/DTG/DTA curves corresponding to the decomposition of the as-prepared samples are shown in Fig. 3 for the TiO_2-Cu 0.5% sample and in Fig. 4 for the TiO_2-Cu 2.0% sample.

The TG curves of TiO_2-Cu 0.5% sample (Fig. 3) shows a total weight loss of 25.7%. On the DTA curve, three heat effects are observed. The endothermal effect at 83°C is attributed to the removal of adsorbed water. The two exothermal effects at 143 °C and 241 °C are assigned to the decomposition of the samples and burning out of organic residues.

The TG/DTA/DTG curves of sample TiO_2-Cu 2.0% (Fig. 4) present more complex decomposition behaviour. The total weight loss is 31% in the 20–200°C temperature range. In the DTA curve, four heat effects are observed. The first effect at 84°C is an endothermal one and is attributed, as in the case of TiO_2-Cu 0.5% sample, to the removal of adsorbed water. The second effect at 122°C is assigned to structural hydroxyls elimination. The exothermal effect at 122 and 177°C is assigned to simultaneous, elimination/oxidation and burning out organic residues. A large effect between 240-345°C is also present, assigned to the burning out of organic residues and crystallization of the resulted amorphous samples.

No weight loss is observed at temperatures higher than 350°C, for neither of the studied samples.

Significant differences regarding the as-prepared samples properties were noticed depending on the amount of dopant (0.5 or 2.0 mol % CuO).

A higher dopant concentration has determined a more complex decomposition. This behavior is associated with the formation of a higher number of different molecular species in the sol-gel solutions before gelation. This fact is supported by the FT-IR spectra that have shown different ratios of organic inorganic components in the studied samples.

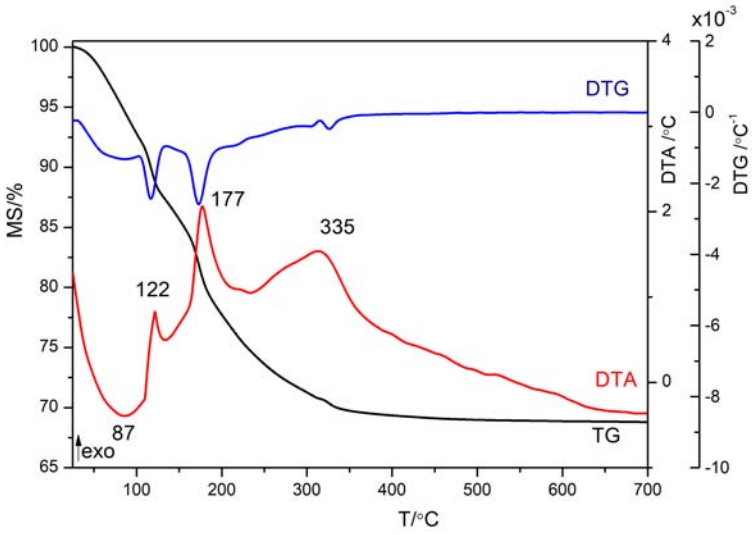

Fig. 4 – TG/DTG/DTA curves of the TiO_2-Cu 2.0% sample.

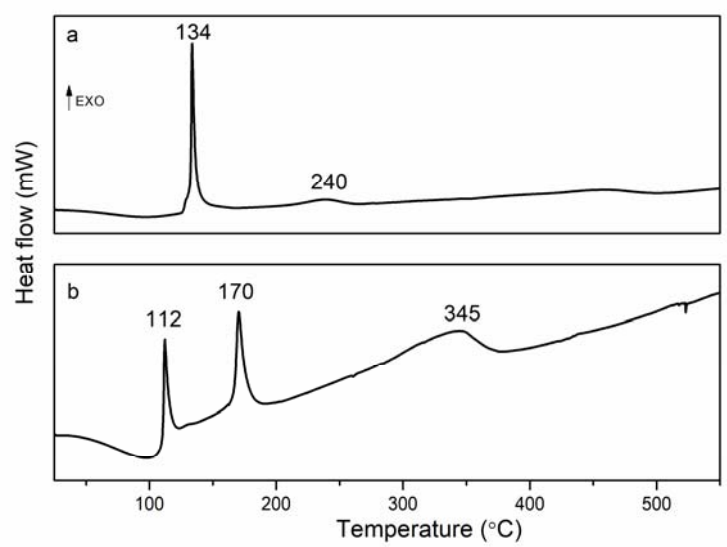

Fig. 5 – DSC curves of the a) TiO_2-Cu 0.5% and b) TiO_2-Cu 2.0% samples

A similar behavior was displayed also by sol-gel prepared TiO_2 powders doped with other ions, namely V.[25-27]

In order to confirm the results obtained by thermal analysis of the TiO_2-Cu 0.5% and TiO_2-Cu 2.0% samples, their thermal behavior was also determined by **DSC measurements**. The DSC results obtained for both samples are presented in Fig. 5.

According to the DSC results, the curves have about the same profile as in the case of DTA results regarding the decomposition behaviour of the samples. In the case of the sample with a small amount of dopant two exothermal effects at 134 and 240°C are observed. For the sample TiO_2-Cu 2% three exothermal effects are present, being associated with water elimination (at 112 ^oC), oxidation and burning out of organic residues (170 ^oC) and crystallization of the anatase phase (345°C).

Based on the TG/DTG/DTA and DSC results, the as-prepared powders were thermally treated at 400 °C for 1 h.

Thermally treated samples (powders)

The **TEM investigation** was performed to gather information about the morphologies of the studied samples. The images of thermally treated samples at 400°C are presented in Figs. 6–8.

The morphology of the two samples is completely different. The TiO_2-Cu (0.5%) sample has irregular or plate aggregates and the TiO_2-Cu

(2.0%) sample is formed mainly by TiO_2 aggregates with a spherical shape. In both samples, the TiO_2 anatase crystallites have similar size between 10 and 15 nm.

In both cases only anatase reflexions are present, as reveled by SAED investigations.

The absence of CuO in the samples indicates its integration in the TiO_2 anatase structure.

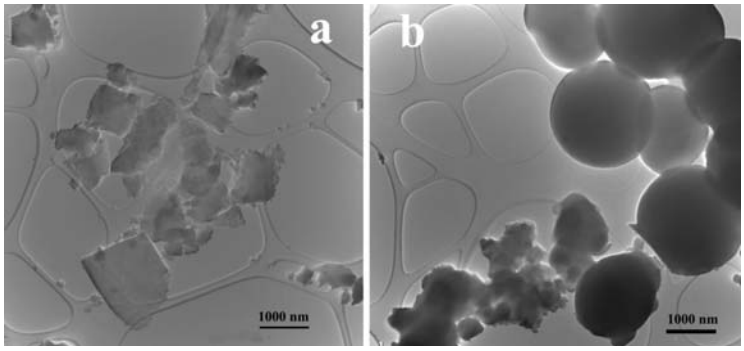

Fig. 6 – Low magnification images of the samples a) TiO_2-Cu (0.5%), b) TiO_2-Cu (2.0%).

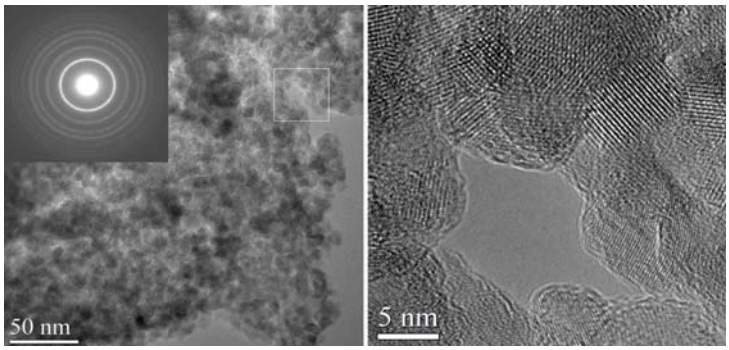

Fig. 7 – TEM image, SAED and HRTEM detail for the sample TiO_2-Cu (0.5%).

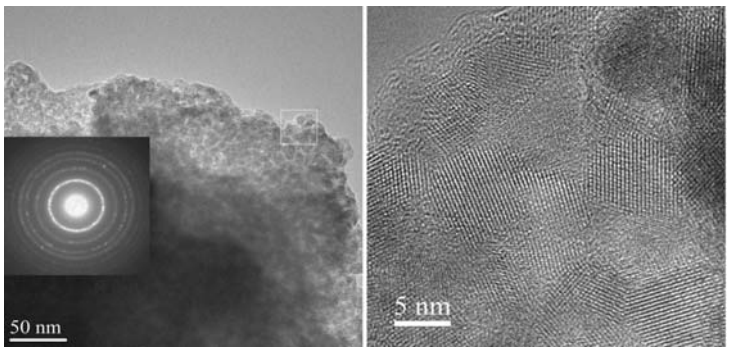

Fig. 8 – TEM image, SAED and HRTEM detail for the sample TiO_2-Cu (2.0%).

The **FT-IR spectra** of Cu doped TiO_2 treated powders are shown in Fig.9.

As compared to the as-prepared samples, the intensity of the characteristic bands assigned to M-O (Ti-O and Cu-O) and M-O-M vibrations is significantly increased.

The other bands assigned to the CO_2 (2350 cm^{-1}) and to the water (1630 cm^{-1}) have much lower intensity and this presence could be due to their adsorbtion from the atmosphere during samples preservation. The band at (1250 cm^{-1}) could be explained by the presence of the organic residues evolved during the thermal treatment of the gels, but retained in low amount on the surface of the sample. The possible retention of the organic species evolved by gels decomposition on the particle surface was previously reported. [32]

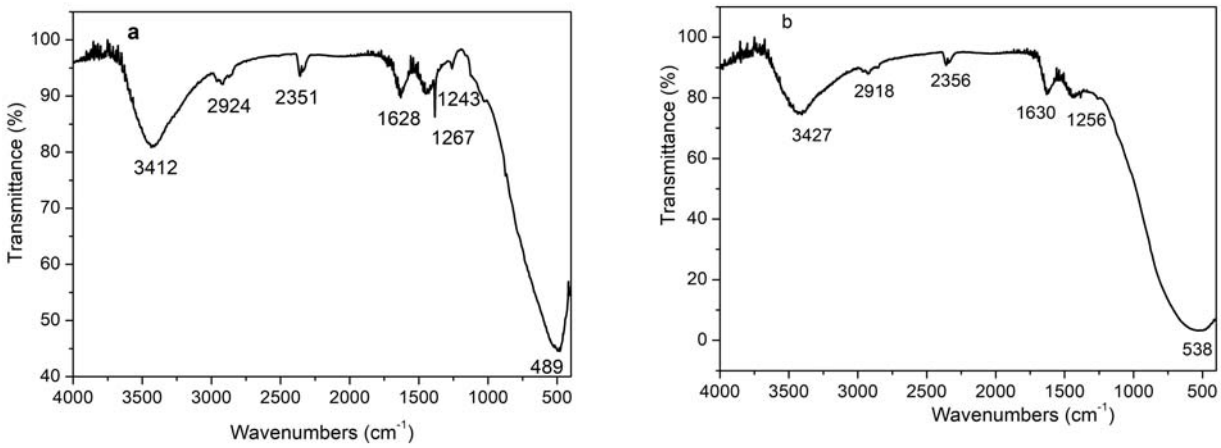

Fig. 9 – IR spectra of the thermally treated Cu-doped TiO_2 powders, a) TiO_2 0.5%, b) TiO_2 2.0%.

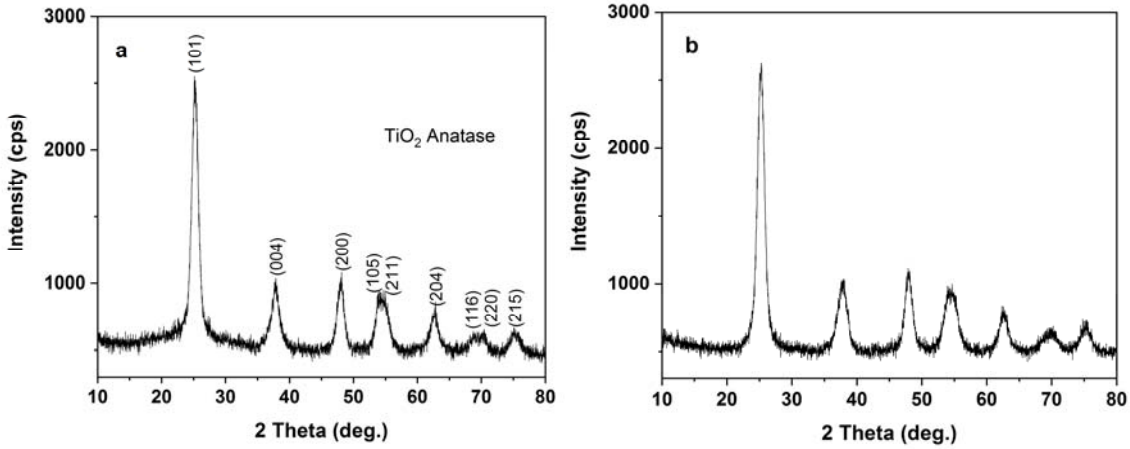

Fig. 10 – The XRD patterns of the samples thermally treated at 400 °C a) TiO_2-Cu 0.5% and b) TiO_2-Cu 2.0%.

The XRD analysis was carried out in order to identify the crystalline structure of the studied samples. The XRD patterns of Cu doped TiO_2 samples are displayed in Fig. 10 a, b.

The reflection peaks indicate the formation of the TiO_2-anatase phase (JCPDS card no. 021-1272). No reflection peaks of the copper crystalline phases (Cu metal, CuO, or Cu_2O) were observed, thus it can be concluded that Cu ions are incorporated within the TiO_2 lattice. For the reflection (101), a slight shift from 25.27° to 25.20° in comparison with the reference (JCPDS 21-1272) is observed. This shift may be due to the interstitial incorporation of Cu ions within the TiO_2 matrix. Interstitial doping generates structural defects in the anatase structure that create internal strain (Table 5).[33]

The average crystallite size estimated by the Williamson method is 59 Å for TiO_2-Cu 0.5% and 57 Å for TiO_2-Cu 2.0%, respectively. The calculated lattice parameters are similar to those from the standard reference. One can assume that due to the differences between the ionic radii of Cu^{2+} (0.73Å) and Ti^{4+} (0.61Å), respectively, Cu ions are mainly located in the interstitial positions of the lattice rather than directly in Ti^{4+} sites.[34]

Table 5

Lattice parameters, strain and crystallite size of the samples

Sample	a=b (Å)	c (Å)	2theta (101)	Crystallite size (Å)	Strain (%)
TiO_2-Cu 0.5%	3.785(3)	9.491(7)	25.20	59(8)	0.8(6)
TiO_2-Cu 2.0%	3.784(2)	9.490(6)	25.21	57(8)	0.9(5)
TiO_2-anatase	3.785	9.514	25.28	-	-

XPS measurements were also performed for the thermally treated samples. In Fig. 11 the XPS spectra are presented. As in the previous samples, the core level spectra of atoms for interest (Ti 2p, O 1s and Cu $2p_{3/2}$) have been deconvoluted using Voigt profiles [30] and in this case we can see that the XPS intensity is improved for the Cu $2p_{3/2}$.

Table 6 presents the binding energies, atomic % values obtained from the deconvolutions and the interpretation of peaks.

For the thermally treated powder samples the XPS spectra of Ti 2p have a more intense peak at ~ 458.4 eV, which is attributed to TiO_2. In this case the O 1s was deconvoluted with 2 components, one at 529,6 eV, which represents the O-Ti, and a small component due to contamination. The Cu $2p_{3/2}$ spectra present a peak at ~ 932 eV, attributed to Cu^+, as it was found in the NIST (National Institute of Standards and Technology) database and in reference. [22]

No shifts were observed for the gel or powder samples, as it was in reference[20]. The XPS analysis shows an oxygen deficit, which seems related to the transformation of Ti^{4+} into Ti^{3+}states as shown in reference.[20] The presence of Cu in TiO_2 and the fact that we obtained a lower percentage of Cu could result from the fact that we are seeing only the small amount of Cu from the surface and Cu substitute Ti. [22]

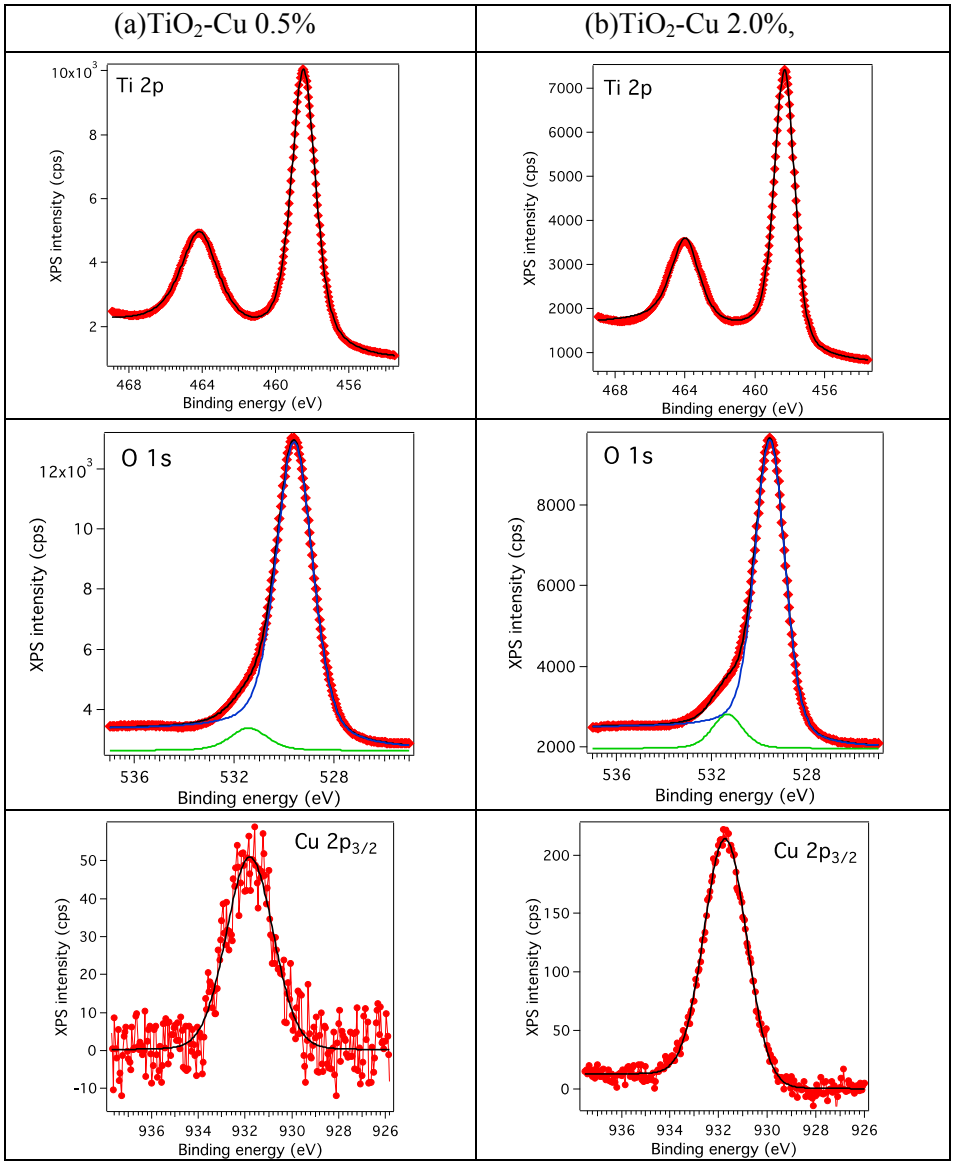

Fig. 11 – XPS spectra of the core level Ti 2p, O 1s and Cu $2p_{3/2}$ for the a) TiO_2-Cu 0.5% and b) TiO_2-Cu 2.0% powders, thermally treated.

Table 6

Main parameters obtained from XPS of the samples whose spectra are presented in Fig. 11

Sample	Element		BE (eV)	% at	Interpretation
TiO_2-Cu 0.5%, powder, thermally treated	Ti 2p	C1	458.46	42.37	TiO_2
	O1s	C1	529.60	53.51	TiO_2 vol.
		C2	531.77	4.07	TiO_2 surface + cont
	Cu 2p3/2	C1	931.80	0.05	Cu(I)
TiO_2-Cu 2.0%, powder, thermally treated	Ti 2p	C1	458.28	37.79	TiO_2
	O1s	C1	529.55	55.49	TiO_2 vol.
		C2	531.28	6.42	TiO_2 surface + cont.
	Cu 2p3/2	C1	931.71	0.32	Cu(I)

Comparing the structure and morphology of the as-prepared samples with that of the thermally treated ones, it could be noticed that the differences observed for the gel samples are maintained also for the powder samples. The differences are correlated with the amount of Cu dopant in the studied samples.

CONCLUSIONS

In the present paper, the preparation by sol-gel method of Cu doped TiO_2 nanometric powders was presented. The influence of the amount of dopant on the thermal behavior as well as on the structure and properties of the resulted nanopowders is also discussed.

The thermal behavior of the as-prepared samples was significantly influenced by the amount of dopant.

The mentioned differences are also maintained in the case of the thermally treated samples.

The results are preliminary and are under further investigation.

Acknowledgements. This work was performed within the frame of the Mobility Project "Reduced semiconductor oxides for TCO, photocatalysis and gas sensing applications, 2019–2021, between the Ilie Murgulescu Institute of Physical Chemistry of the Romanian Academy, Bucharest, Romania and the Research Center for Natural Sciences, Hungarian Academy of Science Research Group of the Hungarian Academy of Science at the Budapest, Hungary. An NRDI K 124212 and an NRDI TNN 16 123631 grants are acknowledged. The research within project No. VEKOP-2.3.2-16-2017-00013 was supported by the European Union and the State of Hungary, co-financed by the European Regional Development Fund. The research reported in this paper was supported by the BME Nanotechnology and Materials Science TKP2020 IE grant of NKFIH Hungary (BME IE-NAT TKP2020).

REFERENCES

1. R.P. Feynman, "There's plenty of room at the bottom: an invitation to enter a new field of physics", In: Gilbert, H.D. (Ed.), Miniaturization, New York, Reinhold, 1959.
2. H.K. Shon, S. Phuntsho, Y. Okour, D.L. Cho, J.B. Kim, S. Na, J.H. Kim, *J. Ind. Eng. Chem*., **2008**, 19, 1–16.
3. Y.C. Nah, I. Paramasivam, P. Schmuki, *Chem.Phys.Chem*., **2010**, 11, 2698–713.
4. M. Tahir, N.A.S. Amin, *Energ. Convers. Manage*., **2013**, 76, 194–214.
5. K. Vijayalakshmi, A. Monamary, *J. Mater.Sci: Mater El*., **2016**, 27, 140–145.
6. B. O'Regan, M. Grätzel, *Nature*, **199**1, 353, 737–740.
7. X. Wei, Z. Yang, S.L. Tay, W. Gao, *Appl. Surf. Sci*., **2014**, 290, 274–9.
8. U.G. Akpan, B.H. Hameed, *Appl. Catal. A-Gen*., **2010**, 375, 1–11.
9. J. Choi, H. Park, M.R. Hoffmann*, J. Mater. Res*., **2010**, 25, 149–58.
10. S.A. Borkar, S.R. Dharwadkar, *J. Therm. Anal. Calorim*., **2004**, 78, 761–7.
11. S.N.R. Inturi, T. Boningari, M. Suidan, P.G.Smirniotis, *Appl. Catal. B-Environ*., **2014**, 144, 333**–**342.
12. M.A. Rauf, M.A. Meetani, S. Hisaindee, *Desalination*, **2011**, 276, 13–27.
13. S. Liu, T. Xie, Z. Chen, J. Wu, *Appl. Surf. Sci*., **2009**,255, 8587–8592.
14. J. Zheng, H. Yu, X. Li, S. Zhang, Appl. Surf. Sci., **2008**, 254, 1630–1635.
15. S.-M. Chang, W.-S. Liu, Appl. *Catal. B-Environ*., **2014**, 156–157, 466–475.
16. A. N. Banerjee, Nanotechnol.Sci. Appl., **2011,** 4, 35–65.
17. A. Khlyustova, N. Sirotkin, T. Kusova, A. Kraev, V. Titov, A. Agafonov, *Mater. Adv.,* **2020**, 1, 1193.
18. R. Dalmis, O. Yasin Keskin , N. Funda Ak Azem, I. Birlik, *Ceram. Int*., **2019**, 45, 21333–21340.
19. B Tryba, J. Orlikowski, R.J. Wro´bel, J. Przepio´rski, A.W. Morawskior, *JMEPEG*, **2015**, 24, 1243–1252.
20. S. Mathew, P. Ganguly, S. Rhatigan, V. Kumaravel, C. Byrne, S. J. Hinder, J.Bartlett, M. Nolan, S. C. Pillai, *Appl. Sci*., **2018**, 8, 2067.
21. Y. Li, S. Peng, F. Jiang, G. Lu,S. Li*, J. Serb. Chem.Soc*., **2007**, 72, 393–402. 22. N. Venkatachalam, M. Palanichamy, B. Arabindoo, V. Murugesan*, Catal. Commun*., **2007**, 8, 1088–1093.
22. R.T. Ako, P. Ekanayake, D. J. Young, J. Hobley, V. Chellappan, A.L. Tan, S. Gorelik, G.S. Subramanian, C.M. Lim, *Appl. Surf. Sci,*. **2015**, *351*, 950–961.
23. L. Samet, K. March, N. Brun, F. Hosni, O. Stephan, R. Chtourou, *Mater. Res. Bull.*, **2018**, 107, 1–7.
24. M. Popa, E. Indrea, P. Pascuța, V. Coșoveanu, I.C. Popescu, V. Danciu, *Rev. Roum. Chim*., **2010,** 55(7), 369–375.
25. I. Stanciu, L. Predoana, J. Pandele-Cusu, S. Preda, M. Anastasescu, K .Vojisavljević, B. Malič, M. Zaharescu, *J. Therm. Anal. Calorim*., **2017**, 130, 2, 639–651.

26. L. Predoana, I. Stanciu, M. Anastasescu, J.M.Calderon-Moreno, M Stoica, S. Preda, M. Gartner, M. Zaharescu, *J. Sol-Gel Sci. Technol*., **2016**, 78, 589–599.
27. I. Stanciu, L. Predoana, C. Anastasescu, D. C .Culita, S. Preda, J. Pandele-Cusu, C. Munteanu, A. Rusu, I. Balint, M. Zaharescu, *Rev. Roum. Chim*., **2014**, 59 (11–12), 919–929.
28. L. Todan, T. Dascalescu, S. Preda, C. Andronescu, C. Munteanu, D.C. Culita, A. Rusu, R. State. M. Zaharescu, *Ceram. Int*., **2014**, 40, 15693–15701.
29. A. Rusu, L. Predoana, S. Preda, J. Pandele-Cusu, S. Petrescu, M. Zaharescu, *Rev. Roum. Chim.,* **2014**, 59, 125–134.
30. M. Teodorescu, J. M. Esteva, R.C. Karnatak, A. El Afif, *Nucl. Instrum. Meth. Phys. Res. A*,, **1994**, **345**, 141–147.
31. C.D. Wagner, L.E. Davis, M.V. Zeller, J.A. Taylor, R.M. Raymond, L.H. Gale, *Surf. Interface Anal.,* **1981**, **3**, 211.
32. A, Szatvanyi, M. Crişan, D. Crişan, A. Jitianu, L. Stanciu, M.Zaharescu, *Rev. Roum. Chim*., **2002,** 47(12), 1255–1259.
33. L.Samet, K. March, O. Stephan, N. Brun, F. Hosni, F. Bessosa, J. Benasseur, R.Chtourou, *J. Alloy. Compd*., **2018**, 743, 175–186.
34. J. Choi, H. Park, M.R. Hoffman, *J. Phys. Chem,* C., **2010,** 114, 783–792.